A Parallel Algorithm for Photomosaicking Based on Mathematical Morphology *

FRANCISCO PINTO ARAÚJO JÚNIOR
NEUCIMAR JERÔNIMO LEITE

DCC/IMECC/UNICAMP
Caixa Postal 6065
13081-970 Campinas-SP-Brazil
[fpintoa, neucimar]@dcc.unicamp.br

Abstract. We define a morphological algorithm for combining two overlapping images into a single one by a process named photomosaicking. The method described here considers the notion of the watersheds of a function to extract global informations of an image denoting the homogeneity between two overlapping regions. Since the basic morphological operations are eminently parallel, the algorithm for photomosaicking can be easily described according to a SIMD programming model.

1. Introduction

Through remote sensing images we can obtain a large number of informations about our planet resources. These informations can be useful for several purposes, such as geologic mapping [Abrams et al. (1985)]; study of the vegetal land cover [Stone et al. (1994)]; agricultural management and planning [Thenkabail et al. (1994)]; distribution and inspection of rural loan through a crop accompaniment; detection of fire active areas; estimation of the agricultural production and management of the available water resources for agricultural needs [Thiruvengadachari (1981)]; control of the water quality stocked in large reservoirs [Verdin (1985)], and so on.

Frequently, for extracting the above informations we need to consider the case in which the study of a region needs to be extended to other neighboring regions represented by different images. In such a case, it becomes necessary to join scenes of the neighboring regions possibly acquired from one or more sensors. The process of composing these images is called *photomosaicking*. Through photomosaicking we can also reconstruct regions which were corrupted by spurious effects such as cloud covering and shadows [Hummer-Miller (1989)].

A photomosaic is defined considering an overlap region between two or more images, in which we detect a join line or seam. This seam indicates where one image ends and the other image begins.

The images which compose the photomosaic should be selected in such a way that aspects as seasonal or time changing, for example, do not compromise the quality of the resultant image. These aspects can generate photomosaics where discontinuous regions, represented by abrupt variations of the pixels, are clearly identified.

In this work we define a parallel method for photomosaicking based on Mathematical Morphology. The parallelism here is inherent to the basic morphological operations which can be easily described according to a SIMD model of computation. As we will discuss elsewhere, by considering the watersheds of a function, the method extracts global information of a correlation image to detect homogeneous areas in which the seam should be defined.

The local aspects of the existing algorithms for photomosaicking [Milgram (1975)], [Milgram (1977)], [Peleg (1981)], [Shiren et al. (1989)] lead to a regular seam with only one pixel per line. Our method defines an irregular and, hence, more realistic seam whose structure depends on global features of the overlap image.

This work is organized as follows. Section 2 presents a brief description of the photomosaicking problems. In Section 3 we introduce some basic notions on Mathematical Morphology. Section 4 describes an algorithm for photomosaicking and illustrates the method. Final comments and conclusions are presented in sections 5 and 6.

2. The Problem Description

The problems related to photomosaicking concern mainly the definition of a seam between two or more overlapping images. These images should be combined into a single one in such a way that the resultant image does not have spurious artificial edges. These artificial edges are represented by a perceptible difference between the points within the region of overlap [Milgram (1977)].

The points of the seam should be such that they

* The work reported in this paper was partially financed by a grant from the GEOTEC-PROTEM project of CNPq-Brazil.

attenuate the discontinuity generated by the photomosaicking. Fig. **1** shows two images and a seam within the overlap region. In a general way, from the line profile of two images, we can say that the points of the seam should be those pixels whose intensity is closer to both line profiles (Fig. **2**). These points define a smooth transition in the neighborhood of the seam.

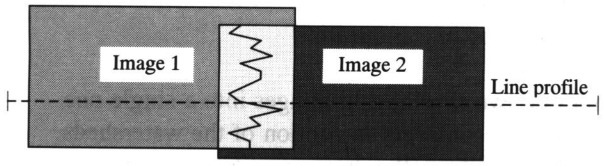

Figure 1. An overlap region and its seam.

The existing algorithms for photomosaicking [Milgram (1975)], [Milgram (1977)], [Shiren et al. (1989)], [Peleg (1981)] define a seam with only one pixel per line (for a horizontal photomosaic) or column (for a vertical photomosaic). Fig. 3 shows an example of a vertical photomosaic in which the seam is defined according to a well-known algorithm presented in [Milgram (1977)]. By considering a monodimensional neighborhood the author defines a seam based on the difference between the points of the two overlapping regions. In defining a horizontal (respectively, vertical) photomosaic the method has the disadvantage of introducing discontinuities in the vertical (respectively, horizontal) direction. An operation for locally smoothing the resultant artificial edge by a ramp function is discussed in [Milgram (1977)]. Obviously, this smoothing operation can represent a loss of information along the neighborhood of the seam.

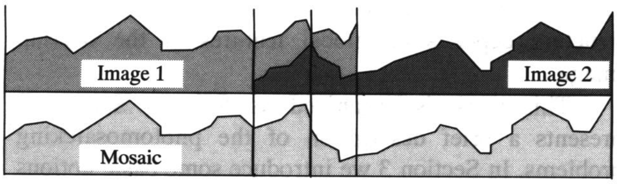

Figure 2. Line profiles of the overlapping images.

In this work we consider the problem of constructing a photomosaic from an *irregular* seam. By irregular we mean a join line which traverses the image in an unknown way, i. e., it can define any path in the overlap region and, consequently, have more than one point per line or column.

Figure 3. A regular photomosaic seam.

As we will see elsewhere, this more natural seam is defined thanks to a powerful morphological operation which segments the images by means of global information.

3. Background

We introduce in this section some basic notions on Mathematical Morphology. For more details see, for example, [Banon-Barrera (1994)], [Serra (1989)], [Haralick et al. (1987)].

Let $f(x)$ be a discrete and binary image, i.e., $\{f(x) \in [0,1]: x \in Z^2\}$, where Z denotes the set of integers. This image can be denoted by a set $\mathbf{X}$ given by $\mathbf{X} = \{x \in Z^2 : f(x) = 1\}$. The complement $\mathbf{X}^c$ of a set $\mathbf{X}$ is given by $\mathbf{X}^c = \{x \in Z^2 : f(x) = 0\}$. The symmetric $\check{X}$ of a set $\mathbf{X}$ is denoted by $\check{X} = \{ -x : x \in \mathbf{X} \}$. The translation $\mathbf{X_u}$ of a set $\mathbf{X}$ by vector u is given by $\mathbf{X_u} = \{ z : z = x + u, x \in \mathbf{X} \}$.

Let the structuring element $\mathbf{B}$ be a finite set. The basic morphological operations are erosion and dilation denoted by

$$X \ominus B = \{ u : B_u \subseteq X \} = \bigcap_{b \in \check{B}} X_b \qquad \text{Eq. 1}$$

and

$$X \oplus B = \{ u : X \cap B_u \neq \varnothing \} = \bigcup_{b \in \check{B}} X_b \qquad \text{Eq. 2}$$

where for a square grid the flat structuring element can be the elementary 4- or 8-connected set as in Fig. 4

Figure 4. 4- and 8-connected flat structuring elements.

The definition of the above operations can be extended to a gray level image g (see, for example, [Haralick et al. (1987)]). For a flat structuring element the erosion and dilation of g by $\mathbf{B}$ can be denoted by

$$(g \ominus \mathbf{B})(x) = \min\{ g(u) : u \in \mathbf{B}\} \text{ and} \qquad \text{Eq. 3}$$

$$(g \oplus B)(x) = \max\{ g(u) : u \in B\} \qquad \text{Eq. 4}$$

The negative or complement, g', of a gray level image g is defined by

$$g' = m - g \qquad \text{Eq. 5}$$

where m is the highest value of g.

Now, let x, y be two arbitrary points of a binary set **X**. We define a geodesic arc of extremity xy as the lower bound of the lengths of the arcs in **X** ending at points x and y. Let us define the number $d_x(x,y)$ as the lower bound, if such arcs exist, and $+\infty$, if not. The function d_x is a distance function called geodesic distance [Lantuejoul-Beucher (1981)], [Lantuejoul-Maisonnenve (1984)].

As stated in [Lantuejoul-Beucher (1981)], all classical morphological transformations (dilation, erosion, skeletonizations etc.) can be defined in the metric space $(\mathbf{X}, d_x)$. For example, if $\mathbf{Y} \subset \mathbf{X}$, points x of **X** such that $\mathbf{B}_x(x, \lambda)$ hits **Y** constitute the λ-dilated set from **Y** in **X** denoted by

$$D^{\lambda}{}_{X}(\mathbf{Y}) = \{ x \in \mathbf{X} : \mathbf{B}_x(x, \lambda) \cap \mathbf{Y} \neq \varnothing \} \qquad \text{Eq. 6}$$

where $\mathbf{B}_x(x, \lambda) = \{ x \in \mathbf{X} : d_x(x,y) \leq \lambda \}$

Practically, the digital geodesic dilation of size n, in Z^2-space, can be obtained from n iterations of a geodesic dilation of size 1, denoted by

$$D^1_x(Y) = (Y \oplus B) \cap X, \qquad \text{Eq. 7}$$

and hence

$$D^n_x(Y) = \underbrace{D^1_x(D^1_x(\ldots D^1_x(Y)\ldots))}_{\text{n times}} \qquad \text{Eq. 8}$$

The structuring element of size 1 can be the 4- or 8-connected set of Fig. **4**.

In the same way we can define the λ-eroded set from **Y** in **X** as the points x of **X** such that $\mathbf{B_X}(x, \lambda)$ is totally included within **Y**.

$$E^{\lambda}{}_{X}(\mathbf{Y}) = \{ x \in \mathbf{X} : \mathbf{B}_x(x, \lambda) \subseteq \mathbf{Y} \} \qquad \text{Eq. 9}$$

3.1 Watersheds of a Function

The watersheds of a function are geometric features which are very useful in picture segmentation [Beucher (1983)]. Let g be a gray level image. The representation of g may be seen as a topographic surface, on which certain features, such as the minima of the image, and its watersheds are of some interest.

An intuitive approach of the watersheds of an image can be the following [Beucher (1983)]. Every minimum of the topographic surface is embedded in a basin. One way to determine the extension of that basin is to flood it. Every time an overflow occurs, a dam can be built on the surface to prevent the overflow. When the dam has drawn a closed contour, we get the boundary of the basin associated to the minimum. The set of all these boundaries is called the watersheds of the image.

The computation of the watersheds is closely related to another morphological operation called thinning [Serra (1989)]. Let $\mathbf{B}_1$ and $\mathbf{B}_2$ be two disjoint subsets of a structuring element **B**. The function p, defined at point x, corresponding to the thinning of the image g by $\mathbf{B} = (\mathbf{B}_1, \mathbf{B}_2)$ can be denoted by

$$p(x) = \begin{cases} \max\limits_{y \in B_2}[g(y)] & \text{iff } \max\limits_{y \in B_2}[g(y)] < g(x) \leq \min\limits_{y \in B_1}[g(y)] \\ g(y) & \text{iff not} \end{cases}$$

Eq. 10

This transformation can be used to define the watersheds of an image. The family of the possible structuring elements used in this operation is the homotopic one. Examples of such elements, for a square grid, are the following (x denotes value 0 or 1).

$$\begin{matrix} 0 & 0 & 0 \\ x & 1 & x \\ 1 & 1 & 1 \end{matrix} \qquad \text{and} \qquad \begin{matrix} x & 0 & x \\ 1 & 1 & 0 \\ 1 & 1 & x \end{matrix}$$

Finally, one can prove that the watersheds of a function are nothing other than the closed arcs of the thinning function [Beucher (1981)].

In the next section we will use the notion of the watersheds of a function to define a seam between two overlapping images.

4. An Algorithm for Photomosaicking

The method described here considers global informations of a correlation image associated to the overlap region of the photomosaic. It is this global feature which allows the definition of a photomosaic through an irregular seam.

Initially, we will consider that the correlation image is simply defined by a pointwise operation denoted by the absolute difference of the pixels in the two overlapping regions. In such a way, we define an image whose low value pixels represent strong *candidates* for the seam.

The correlation image can be seen as a topographic surface containing "peaks" and "valleys", i. e., points whose height denotes regions of low or high correlation. Thus, we can use the notion of the watersheds of a function to segment the correlation image, and find points which belong to the valleys (regions of high correlation) of this image. Here, to detect the watersheds relative to these valleys, we need consider the negative of the correlation image.

The algorithm for photomosaicking consists mainly of two steps :

1. Definition of the watershed lines of the

correlation image.

2. Definition of a two-phase image indicating the points relative to each side of the photomosaic.

The watersheds can be defined according to Eq. 10. Fig. 7 shows the watersheds of the correlation image relative to the overlap region of the images in Fig. **5** and 6 (for a vertical seam).

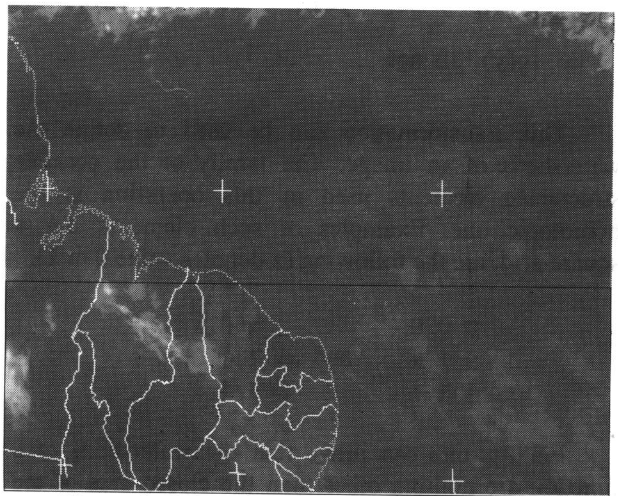

Figure 5. Uppermost side of the photomosaic.

As we can see in Fig. 7, the segmentation by watersheds leads to a super-segmented image with several optional paths traversing the overlap region. Step 2 above consists then in eliminating these redundant paths and defining a two-phase image in which each phase is related to one side of the photomosaic (this two-phase image indicates where one image ends and the other image begins).

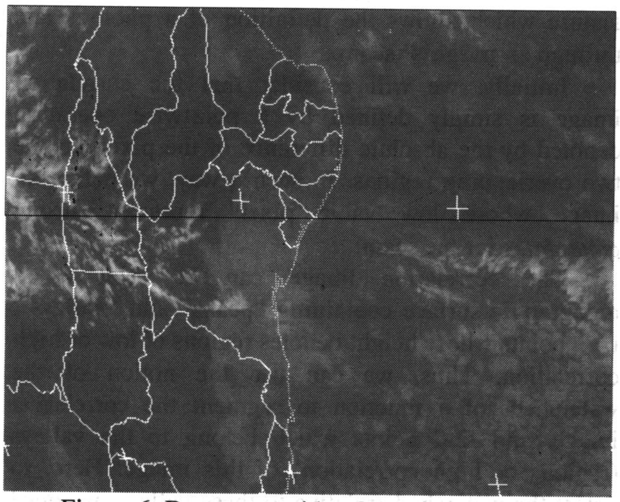

Figure 6. Downmost side of the photomosaic.

Morphologically, this two-phase image can be defined by means of the geodesic transformations discussed in section 3. The approach consists in dilating a marker from the leftmost (uppermost) edge of the segmented image and another marker from its rightmost (downmost) edge, for a horizontal (vertical) photomosaic. After the markers dilation, watershed lines which are not between two different phases can be eliminated. This operation stops when both labels meet a watershed line separating them. Remark that, in this case, the only criterion for detecting the final seam is symmetry (we consider that the geodesic dilation of the two markers is executed in parallel and hence the final seam tends to the middle of the segmented image).

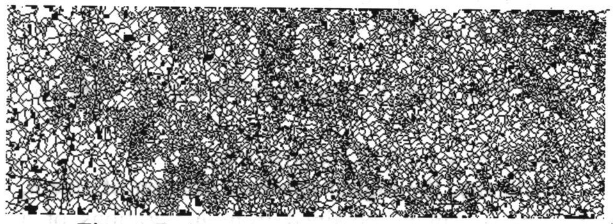

Figure 7. An example of watershed image.

Let, for a vertical photomosaicking, $\partial\mathbf{U}$ and $\partial\mathbf{D}$ be the marker sets corresponding to the uppermost and downmost edges of a binary image **W.** This image indicates the points of the correlation image which belong to the watershed lines, namely the points which are greater than zero. To these sets we associate labels U and D, respectively.

The geodetic dilation (Eq. 1) of the markers $\partial\mathbf{U}$ and $\partial\mathbf{D}$ in image **W** can be denoted by

$$\mathbf{G} = D^{\infty}{}_{Wc}(\partial\mathbf{U}) \cup D^{\infty}{}_{Wc}(\partial\mathbf{D}), \qquad \text{Eq. 11}$$

Informally, $D^{\infty}(.)$ means execution of the geodesic dilation until stabilization. Since $\partial\mathbf{U}$ and $\partial\mathbf{D}$ are disjoint sets, their geodesic dilation can be executed in parallel. A two-phase image *p* containing labels U and D is such that

$$p(x,y) = \begin{cases} U, \text{if } [(x,y) \in G] \subset D^{\infty}_{W^c}(\partial U) \\ D, \text{if } [(x,y) \in G] \subset D^{\infty}_{W^c}(\partial D) \\ 0, \text{if not} \end{cases} \qquad \text{Eq. 12}$$

i.e., the pixels of the image **G** at position (x,y) indicate the points of the two-phase image having value U (if the corresponding points in **G** belong to the dilated set $\partial\mathbf{U}$) or D (if the corresponding points in **G** belong to the dilated set $\partial\mathbf{D}$). The Fig. 8 illustrates the geodesic dilation of a marker set $\partial\mathbf{U}$ in a set $\mathbf{X}^c$. We consider here that the foreground (black pixels) has value 1 and is 8-connected, and the background (white pixels) has value 0 and is 4-connected (the structuring element **B** used in the geodesic dilation is the 4-connected set as in Fig. 4).

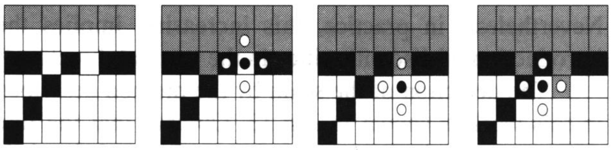

Figure 8. Geodesic dilation.

After this step the points $(\mathbf{G} \oplus \mathbf{B}) \setminus \mathbf{G}$ of the image **W** which are not between two regions, labeled with U and D, are eliminated and in such a case we can continue executing the operations denoted by Eq. 11 and 12. These operations are repeated until only two phases, namely U and D, remain in the image *p*. The line between these two subsets constitutes the seam of the photomosaic.

Informally, the definition of the two-phase image consists simply in scanning the segmented image and propagating, along points which do not belong to the watershed lines, the labels U and D related to the uppermost and downmost edges. The propagation continues until a line separating the two phases is defined. Fig. 7 shows the watershed lines of the overlap regions in Figs. 5 and 6.

The way the method eliminates the optional paths does not take into account the height of the watersheds. In this case we can eliminate good paths, corresponding to very low valleys, due to the fact that they are close to the edges $\partial\mathbf{U}$ or $\partial\mathbf{D}$.

Studies concerned with the human visual system have shown that the total range of intensity levels we can discriminate simultaneously is rather small. Only one to two dozen of gray levels are detectable at any one point in an image [Gonzalez-Wintz (1987)]. Let us suppose that our image has 256 gray levels. Then, in the worst case, we can discriminate about 10 of these gray levels in a small neighborhood of a pixel.

We use this result to eliminate points of the watershed lines which are less than a certain threshold (recall that the watershed image is based on the negative of the correlation image). Obviously, the elimination of a point of a watershed line corresponds to a further elimination of this line. In our case, as the correlation image is defined by pointwise absolute differences of the two overlap images, the threshold should be the half of the value considered above.

The extension of the method for photomosaicking can be described by the following steps (for a vertical photomosaic).

1 Define a binary image **W** representing the points of the watershed lines of a correlation image (the negative of it).
2 Propagate, in parallel, the labels U (from the uppermost edge) and D (from the downmost edge) until a watershed line is found.
3 Repeat until only one watershed line separating two U and D labeled regions is found.
   - eliminate the watershed lines whose points in the correlation image exceed a certain threshold (5, in our case).
   - propagate downwards and upperwards the labels U and D, respectively.
   - if stabilization then
     - eliminate one current watershed line and continue the propagation of labels U and D.

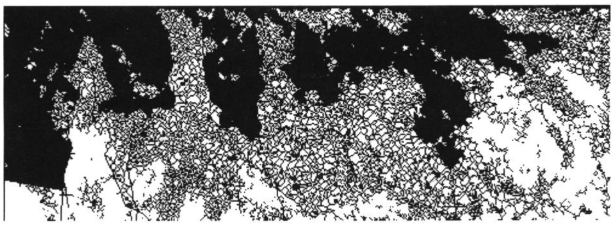

Figure 9. Watershed image after the 1th stabilization.

Fig. 9 shows the propagation of two labels in a image **W** until the first stabilization. This image corresponds to the watershed lines of the overlap regions in Figs. 5 and 6. Fig. 10 shows the seam over the final photomosaic.

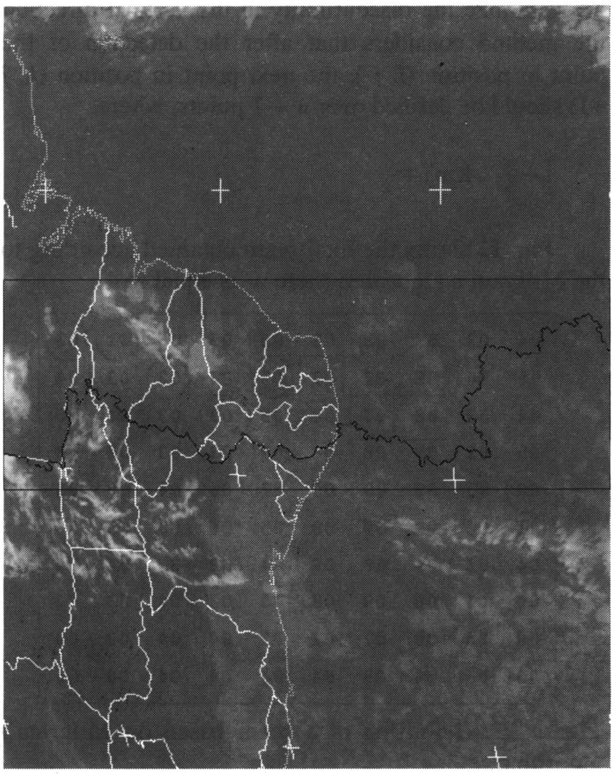

Figure 10. Morphological mosaic.

5. Final Comments

To point out the difference between the method discussed here and those which take into account only local properties of the pixels, let us consider, for a vertical photomosaic, the image in Fig. **11**. It represents the absolute differences between the points in the overlapping images (the polygon in the figure indicates a region of low correlation).

04	03	03	08	08	03	05	06	01	03
05	04	08	07	07	03	04	02	03	04
04	03	08	07	08	05	03	03	04	00
05	02	09	08	08	07	03	03	02	03
00	03	09	09	09	07	06	04	00	05
01	06	09	08	08	05	06	00	05	06
04	03	09	08	08	04	02	01	04	06
09	01	08	08	08	03	03	04	03	07
06	03	08	07	07	03	04	04	02	08
06	06	04	03	04	04	04	04	08	06

Figure 11. An image of absolute differences.

The well-known algorithm discussed in [Milgram (1977)] is a good example for illustrating such a difference. Basically, it creates a seam with one point per column defined as the lowest value in each column. To minimize the discontinuity in the vertical direction the method considers that after the detection of the point in position (i, j), the next point in position $(k, j+1)$ should be defined over $w + 1$ points, where

$$i - \frac{w}{2} \leq k \leq i + \frac{w}{2}$$

Fig. **12** shows the final seam obtained according to the Milgram's algorithm (here w is equal to 4).

04	03	03	08	08	03	05	06	01	03
05	04	08	07	$\boxed{07}$	03	04	02	03	04
04	03	$\boxed{08}$	$\boxed{07}$	08	05	03	03	04	00
05	02	09	08	08	07	03	03	02	03
00	03	09	09	09	07	06	04	00	05
01	06	09	08	08	05	06	00	05	06
04	03	09	08	08	04	02	01	04	06
09	01	08	08	08	03	03	04	03	07
06	03	08	07	07	03	04	04	02	08
06	06	04	03	04	04	04	04	08	06

Figure 12. Definition of a seam based on Milgram's algorithm.

Remark that in this case some low correlation points (points within small squares) belong to the seam. Obviously, we can avoid this problem by increasing the size w of the monodimensional neighborhood. Nevertheless, in practice, this increasing implies the introduction of discontinuities in the vertical direction.

The detection of the seam by the method described in this work is shown in Fig 13. Observe that the line does not cross the low correlation region and that it is connected. The connectivity criterion is guaranteed by the watershed algorithm which is a homotopic operation.

04	03	03	08	08	03	05	06	01	03
05	04	08	07	07	03	04	02	03	04
04	03	08	07	08	05	03	03	04	00
05	02	09	08	08	07	03	03	02	$\boxed{03}$
00	03	09	09	09	07	06	04	$\boxed{00}$	05
$\boxed{01}$	06	09	08	08	05	06	$\boxed{00}$	05	06
04	$\boxed{03}$	09	08	08	04	02	$\boxed{01}$	04	06
09	$\boxed{01}$	08	08	08	03	$\boxed{03}$	04	03	07
06	$\boxed{03}$	08	07	07	$\boxed{03}$	04	04	02	08
06	06	$\boxed{04}$	$\boxed{03}$	$\boxed{04}$	04	04	04	08	06

Figure 13. Definition of a seam based on the watersheds of a function.

6. Conclusion

We have proposed a new algorithm for photomosaicking based on a very powerful morphological operation used for segmenting images. By taking into account global informations of the overlap region, the watershed algorithm defines a seam which is connected, irregular and thus more realistic than the existing methods for photomosaicking. Furthermore, due to the parallel nature of the morphological operations, the method reported here can be easily described according to a SIMD model of computation.

Interesting extensions to this work concern the definition of other correlation criteria, and the detection of a line having the lowest topographic cost in the watershed image.

7. References

C. Lantuejoul, F. Maisonnenve, *Geodesic Methods in Image Analysis*, Pattern Recognition, 17, 1984, pp. 177-187.

C. Lantuejoul, Serge Beucher, *On the use of Geodesic Metric in Image Analysis*, J. of Microscopy, 121, 1981, pp. 39-49.

David L. Milgram, *Computer Methods for Creating Photomosaics*, IEEE Trans. Comp., November

1975, pp. 1113-1119.

David L. Milgram, *Adaptive Techniques for Photomosaicking*, IEEE Trans. Comp., November 1977, pp. 1175-1180.

G. J. F. Banon, J. Barrera, *Bases da Morfologia Matemática para Análise de Imagens Binárias*, IX Escola de Computação, July 24-31, 1994, Recife, PE, Brazil.

James P. Verdin, *Monitoring Water Quality Conditions in a Large Western Reservoir with Landsat Imagery*, PE&RS, March 1985, pp. 343-353.

Jean Serra, *Image Analysis and Mathematical Morphology*, Vol. 1, Academic Press, 1981

M.Abrams, A. Blusson, V. Carrere, T. Nguyen, Y. Rabu, *Image Processing Applications for Geologic Mapping*, IBM Journal Res. Devel., Vol. 29, March 1985, pp. 177-187.

Prasad S. Thenkabail, Andrew D. Ward, John G. Lyon, Carolyn J. Merry, *Thematic Mapper Vegetation Indices for Determining Soybean and Corn Growth Parameters*, PE&RS, April 1994, pp. 437-442.

Rafael C. Gonzalez, Paul Wintz, *Digital Image Processing*, 2nd Edition, 1987, Addison-Wesley.

Robert M. Haralick, Stanley R. Sternberg, Xinhua Zhuang, *Image Analysis Using Mathematical Morphology*, IEEE Transactions on Pattern Analysis and Machine Intelligence, July 1987, pp. 532-550.

Serge Beucher, *Ligne de Partage des Eaux. Comment l'expliciter en Termes de Transformation Fonctionnelle*, C.G.M.M., n. 699, May 1981.

Serge Beucher, *Extrema of Grey-Tone Functions and Mathematical Morphology*, Fontainebleua, 1983.

Shmuel Peleg, *Elimination of Seams from Photomosaics*, IEEE Conference on Pattern Recognition and Image Processing, 1981

Suzanne Hummer-Miller, *A Digital Mosaicking Algorithm Allowing for an Irregular Join "Line"*, PE&RS, January 1989, pp. 43-47.

S. Thiruvengadachari, *Satellite Sensing of Irrigation Patterns in Semiarid Areas : An Indian Study*, PE&RS, October 1981, pp. 1493-1499.

Thomas A. Stone, Peter Schlesinger, Richard A. Houghton, George M. Woodwell, *A Map of the Vegetation of South America Based on Satellite Imagery*, PE&RS, May 1994, pp. 541-551.

Yang Shiren, Li Li and Gao Peng, *Two-Dimensional Seam-Point Searching in Digital Image Mosaicking*, PE&RS, January 1989, pp. 49-53.